

# Analysis of anode current distribution in aluminum electrolysis cell based on equivalent circuit numerical simulation

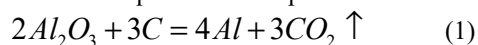
Yifan Wang<sup>1</sup>, Peixin Zhou<sup>1</sup>, Jun Tie<sup>1\*</sup>

<sup>1</sup>School of Mechanical and Materials Engineering, North China University Of Technology, 100144, P.R. China

**Abstract:** The development of modern industrial aluminum reduction cell towards the direction of higher line current and more anodes. The distribution of anode current and the stability of the fluid in reduction cell are directly affected by the busbar configuration. In this paper, a simulation model of the multi-loop equivalent circuit of aluminum electrolysis cell was established by using MATLAB/Simulink, and the distribution characteristics of anode current under three different current risers were analyzed. The results show that with the increase of the number of terminals, the cell voltage decreases and anode current distribution is more uniform. The anode current is positively correlated with the distance from the terminal and the current of the nearest column busbar.

## 1. Introduction

At present, industrial aluminum production adopts the Hall-Héroult electrolysis method invented in 1886, and its main production equipment is aluminum electrolysis cell. The total reaction equation for the production is:



In the production process, if a certain anode current is too large, the local anodic effect will occur when the alumina concentration is low, emitting strong greenhouse gases [1] perfluorocarbons (PFCs), forming serious environmental problems and reducing the efficiency of electrolytic current, so balanced anode current distribution is one of the goals of aluminum production. In actual production, the cell voltage and line current can reflect the overall operating condition of the electrolysis cell, and the anode current can provide an insight into the localized anodic dynamic behavior, so the equivalent circuit model can be established according to the circuit structure of the cell, and then the model can be solved by using Kirchhoff's law. Finally, the current on the conductor such as anodes and column bus can be given in real time to evaluate the local operating state of the electrolysis cell.

Cheung C Y et al. [2] gave a single anode path resistance model, measured and analyzed the current of a newly replaced anode, and divided it into three stages according to the rate of the current uptake. Wang Y et al. [3] studied the dynamic simulation of the anode current field equivalent circuit of the reduction cell, established the equivalent circuit model of the anode current distribution, and further studied the variation characteristics of the current field. Yao Y et al. [4] presents an approach to estimate in real time the alumina concentration distribution in an aluminum reduction cell based on individual anode current measurements. Dion L

et al. [5] discussed a model of non-homogenous alumina and current distribution in an aluminum electrolysis cell and used it to predict low-voltage anode effects. Guérard S et al. [6] used Matlab to establish a transient mathematical model of anode current and anode-cathode distance distribution, and discussed the effects of anode self-change, anode height, anode section, and disappearance of the slots on current efficiency.

In this paper, the circuit structure of the cell is simulated by using the equivalent circuit method. Matlab/Simulink was used to establish an equivalent circuit model that conforms to industrial production. Using this model, the influence of different busbar configurations on the current distribution and cell voltage is studied.

## 2. Parameter and modeling

Taking a 500kA aluminum reduction cell as an example, the equivalent circuit model is established in Simulink, and the main model parameters are shown in Table 1.

**Table1** Model parameters

Parameter	Value
Line current (kA)	500
Cell voltage (V)	4.0
ACD(cm)	4.5
Al <sub>2</sub> O <sub>3</sub> (wt%)	3.88
Anode size (mm)	1770*770*660
Electrolyte temperature (K)	1223
Anode carbon resistance (μΩ)	38

The cell voltage can be regarded as composed of the reaction equilibrium potential, reaction overvoltage, electrolyte voltage, bubble voltage, anode carbon voltage, cathode voltage, and external voltage drop through cell structure, expressed as resistance and anode current [4].

\*email: [tiejun@ncut.edu.cn](mailto:tiejun@ncut.edu.cn)

$$U_{cell} = E_{re} + (R_{ov} + R_{ACD} + R_{bu} + R_a)I + U_c + U_{ex} \quad (2)$$

The little voltage drop generated by the metal pad is ignored in the calculation of the cell voltage, and it is assumed that the overvoltage is caused by the anode reaction overvoltage [1]. The reaction equilibrium potential can be calculated as [7]:

$$E_{re} = E^0 - \frac{RT_{bath}}{12F} \ln \frac{1}{\alpha Al_2O_3} \quad (3)$$

Where  $E^0$  is the standard potential,  $T_{bath}$  is the bath temperature,  $\alpha Al_2O_3$  is the activity of alumina,  $F$  is Faraday constant and  $R$  is the gas constant. The anode over resistance satisfy the equation (4).

$$R_{ov} = \frac{U_{ov}}{I} = \frac{a + b \lg i_a}{I} \quad (4)$$

Where  $a$  is the Tafel constant,  $b$  is the Tafel slope,  $i_a$  is the current density and  $I$  is anode current. The electrolyte resistance and the bubble voltage is expressed as follows [1]:

$$R_{ACD} = \frac{ACD - b_b}{S \cdot \kappa} + \frac{b_b - d_b}{S \cdot \kappa (1 - 0.02 C_{Al_2O_3})^{1.5}} \quad (5)$$

$$U_{bu} = IR_{bu} = I \frac{d_b}{\kappa (1 - 1.26 f_s) S} \quad (6)$$

Where  $ACD$  is the anode-cathode distance,  $\kappa$  is the electrolyte conductivity,  $b_b$  is the thickness of bubble,  $d_b$  is the thickness of the single-layer bubble,  $f_c$  is the bubble coverage rate of the anode surface,  $S$  is the effective area, and  $C_{Al_2O_3}$  is the alumina concentration.

Since the resistance of anode carbon, rod, steel yoke, cathode carbon, cathode steel rod and external conductor in a short time are almost unchanged, the anode resistance  $R_a$ , cathode voltage  $U_c$ , external voltage drop  $U_{ex}$  can be regarded as a fixed value. According to the voltage composition of the cell and its conductive structure, the aluminum reduction pots can be equivalent to a multi-loop equivalent circuit.

## 2.1. Construction of nonlinear resistance module

It can be seen from the analysis of cell voltage composition that the anode over resistance, electrolyte resistance and bubble resistance are all nonlinear resistors, and their values are affected by many parameters such as electrolyte components, which are considered as interelectrode equivalent resistances [8]. In Simulink, the controlled voltage source module can be used to implement the function of nonlinear resistance. The bubble resistance is taken as an example.

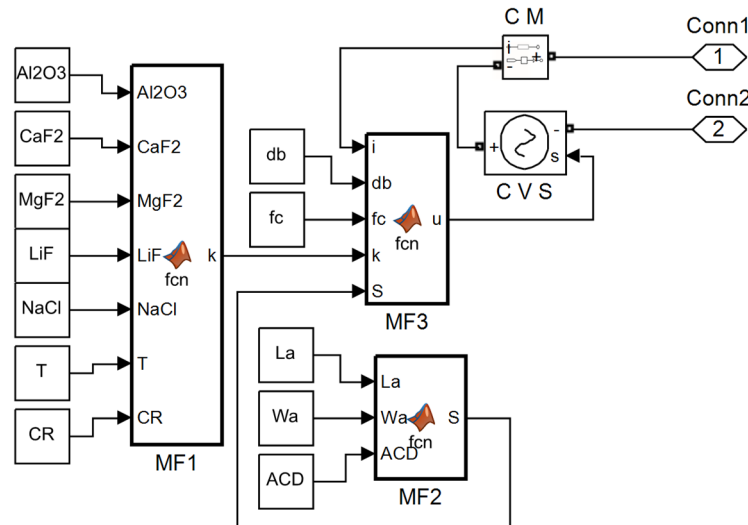
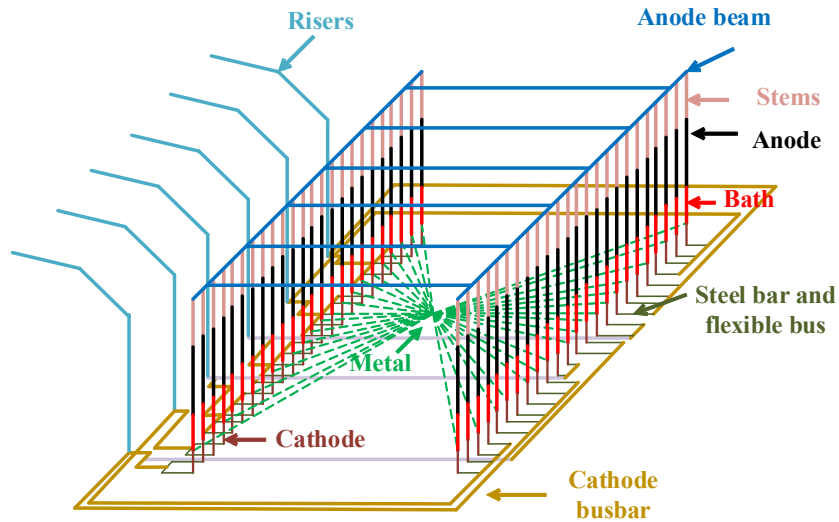


Fig 1 Bubble resistance module  $R_{bu}$

As shown in Fig 1, MF1, MF2, and MF3 are MATLAB function modules, which is used to write the bubble voltage function shown in equation (6) to control the voltage source CVS to represent the bubble resistance. CM is the current measurement module, and its terminal  $i$  outputs the current value of the circuit. Conn1 and Conn2 are connection ports for connecting external circuits. The remaining nonlinear resistors and equilibrium potential can also be constructed one by one in this way, and the anode-related resistance module can be obtained by connecting them in series [2-3] and packaging them.

## 2.2. Equivalent circuit model

Take the asymmetrical six terminals busbar configuration [9] as an example, the equivalent resistance corresponding to the cell is shown in Fig 2. Considering the metal pad as an equipotential [6] and bounded by this, the cell can be divided into the anode section above the molten aluminum and the cathode section below, and the main difference between the different busbar configurations is the cathode part.



**Fig 2** Asymmetrical six terminal busbar configuration

The current flows from different anode rods to anode carbon, then through the electrolyte and metal pad, to the cathode carbon, and finally through the cathode busbar to the next cell. By connecting the current source and each

resistor module according to the cell structure, asymmetric six terminals equivalent circuit models obtained are shown in Fig 3.

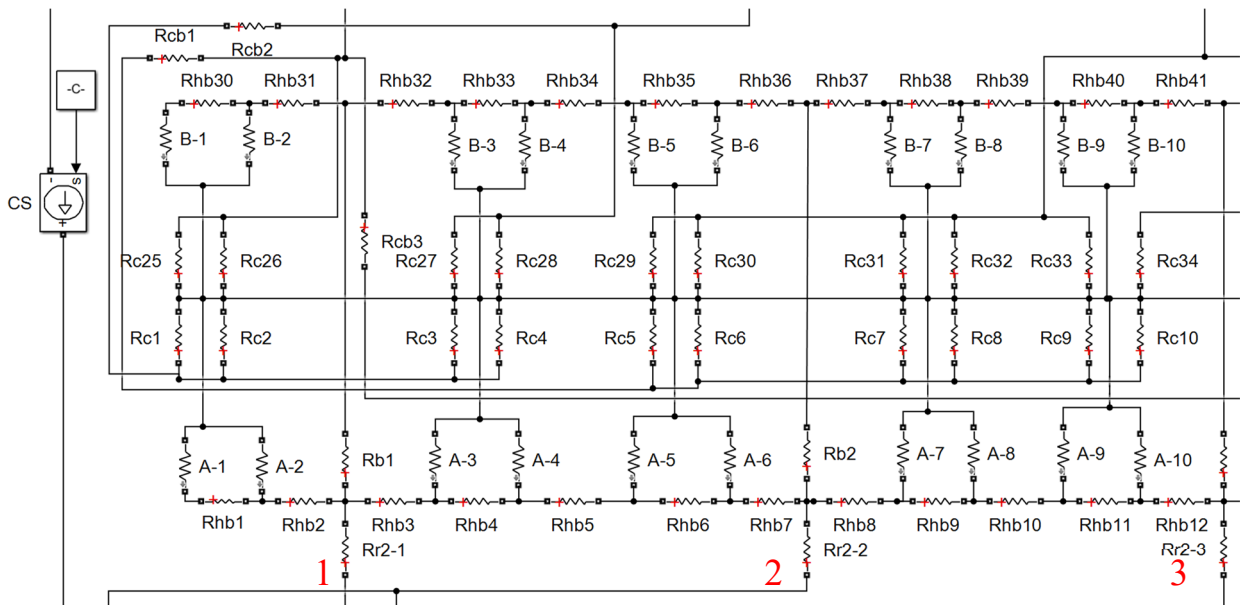


**Fig 3** Part of the asymmetric six terminals equivalent circuit model

As shown in Fig 3, a constant current source CS is used to represent the line currents, and each anode-related resistance has a corresponding number, for example, A-1 is the first anode on the side A. In this model, in addition to the reduction pot to be studied, the cathode part of the upstream cell and the anode part of the downstream cell are also included. The current flows simultaneously from the cathode part of the upstream cell through six risers into the cell under study. The cell equivalent circuit of single terminal and two terminals <sup>[10]</sup> can be obtained by the same method.

### 3. Results and discussion

The constant current of 500kA is input in the model. The anode current magnitude and distribution in the three bus configurations are shown in Fig 4 (a), (b), and (c). It can be seen that regardless of the bus arrangement, the anode current on side A is slightly higher than that on side B, but the difference is not more than 0.5% ,which is consistent with the research of Cao X et al <sup>[11]</sup> .This is because the anode voltage on side B is lower than that on side A after being shared by the connecting bus when every anode-related resistance is almost the same.

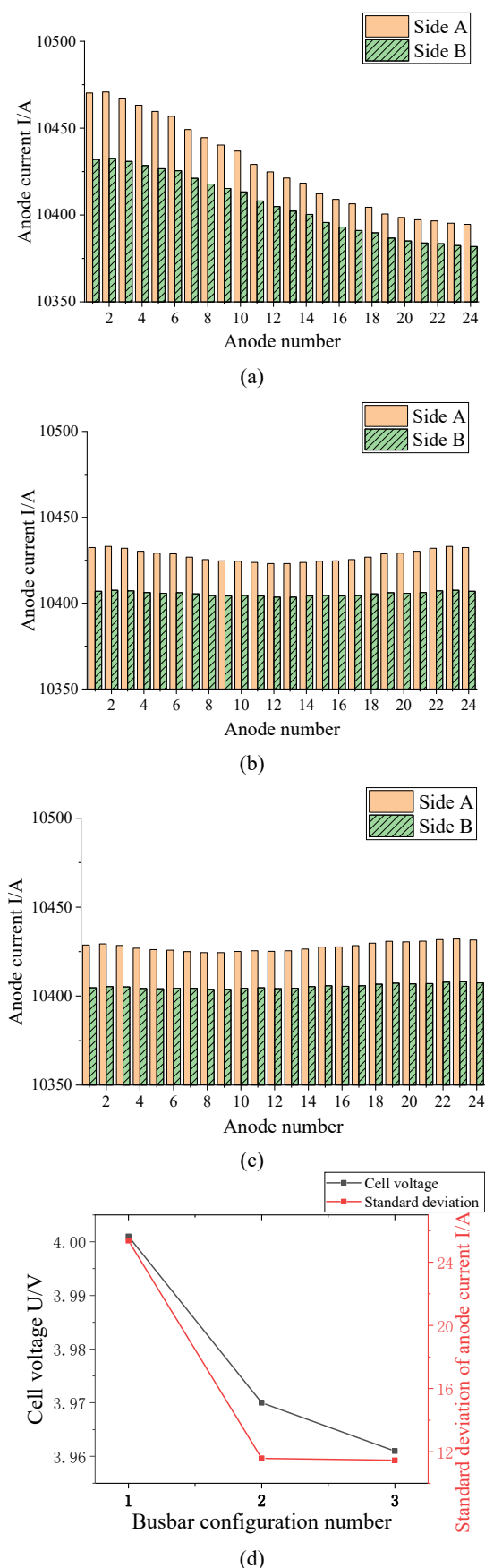


**Fig 4** Anode current distribution and cell voltage variation in different current risers  
 (a) Single terminal; (b) Two terminals; (c) Six terminals; (d) Relation between cell voltage and standard deviation of anode current and number of terminals respectively

The anode currents on both sides of A and B have the same distribution. From Fig 4(a), it can be seen that the farther the anode is from the terminal, the smaller the anode current, from the maximum 10470A to the minimum 10381A. In(b), anode current decreases first and then grows with the increase of the anode number, and the current at B-12, which is farthest from the two terminals, is the minimum 10403A. In (c), the anode A-8 and A-20 are the same distance from the nearest terminal, but the current of A-8 is the minimum on side A, which is due to the smallest current at the nearest terminal 2 to A-8.

The three busbar configurations are numbered in order of the number of terminals from less to more, and the cell voltage and standard deviation of anode current with different configurations is shown in Figure 4(d). The cell voltage of six terminals is about 1% lower than that of single terminal. As the number of terminals increases, the cell voltage and the standard deviation of anode current declines, and the anode current distribution is more uniform.

#### 4. Conclusion

In this paper, the conductor of aluminum electrolysis cell is equivalent to the corresponding resistance, and the effects of three busbar configurations on anode current distribution and cell voltage is simulated.

(1) Among the three busbar configurations, the anode current on A side is slightly larger than the B, and the anode current on both sides has the same distribution trend.

(2) With the increase of the number terminals, cell voltage showed a downward trend, and anode current distribution was more uniform, among which the asymmetric six terminals model had the most balanced anode current distribution.

(3) The anode current is positively correlated with the distance from the terminal and the current magnitude of the nearest column busbar.

#### Acknowledgements

The authors would like to acknowledge support from the National Key R&D Program of China under Grant 2022YFB3304900.

#### References

[1] Feng N. Aluminium electrolysis [M]. Beijing:Chemical Industry Press, 2006.  
 [2] Cheung C Y, Menictas C, Bao J et al. Characterization of Individual Anode Current Signals in Aluminum Reduction Cells[J]. Industrial & Engineering Chemistry Research, 2013, 52(28): 9632-9644.  
 [3] Wang Y, Tie J, Sun S et al. Testing and Characterization of Anode Current in Aluminum Reduction Cells[J]. Metallurgical and Materials Transactions B, 2016, 47(3): 1986-1998.

- [4] Yao Y, Cheung C Y, Bao J, Skyllas-Kazacos M, Welch BJ, Akhmetov S. Estimation of spatial alumina concentration in an aluminum reduction cell using a multilevel state observer[J]. *AIChE Journal*, 2017, 63(7): 2806-2818.
- [5] Dion L, Kiss L, Poncsak S et al. Simulator of Non-homogenous Alumina and Current Distribution in an Aluminum Electrolysis Cell to Predict Low-Voltage Anode Effects[J]. *Metallurgical & Materials Transactions B*, 2018, 49(2): 737-755.
- [6] Guérard S, Côté P. A Transient Model of the Anodic Current Distribution in an Aluminum Electrolysis Cell[C]. *TMS Light Metals*, 2019: 595-603.
- [7] Haupin W . Interpreting the Components of Cell Voltage[M]. John Wiley & Sons, Ltd, 2013.
- [8] Tie J, Li C, Zhao R T et al. A digital twin control system for aluminum electrolysis cell [P]. CN:202011588070.5, 2021-11-30.
- [9] Zhang Q S , Yang X D , Liu Y F et al. An Asymmetrical Six terminals Busbar Configuration for Large Aluminum Electrolysis Cells [P].CN:200810012376.9,2010-01-20.
- [10] Qiu Y. Development and outlook for busbar arrangement of aluminum reduction pots [J].*Light Metals*, 2019,(9):36-39.
- [11] Cao X, Zhang Q, Zhao Z et al. Study on the evolution rule of interface deformation and anode current distribution in aluminum pots during anode changing[J]. *Light Metals*,2021,(6):20-28.